Breakthrough Curves for Fixed-Bed Adsorbers: Quasi-Lognormal Distribution Approximation

Guo-hua Xiu and Tomoshige Nitta
Dept. of Chemical Engineering, Osaka University, Osaka 560, Japan

Ping Li and Ge Jin
Dept. of Chemical Engineering, Shenyang Institute of Chemical Technology, Shenyang 110021, China

The quasi-lognormal distribution (Q-LND) approximation was used to predict breakthrough curves in fixed-bed adsorbers for a linear adsorption system with axial dispersion, external film diffusion resistance, and intraparticle diffusion resistance for slab-, cylindrical-, and spherical-particle geometries. The exact solution and parabolic profile approximation were also obtained for different particle geometries. Numerical results show that the Q-LND approximation is a simple and handy solution. It predicts breakthrough curves with an accuracy comparable to the parabolic-profile approximation over a wide range of parameters; compared with the latter, it only takes less than one hundredth the computation time and does not have a convergence problem in numerical calculations. A criterion for the applicability of the Q-LND approximation is suggested. The effect of particle geometries on the breakthrough curves is discussed. A criterion is also provided for the Q-LND approximation to explore the conditions where one should consider this effect on breakthrough curves.

Introduction

Various expressions for exact analytical solutions of breakthrough curves for fixed-bed adsorbers have been derived by many authors (Rosen, 1952; Masamune and Smith, 1965; Rasmuson and Neretnieks, 1980). The mathematical models become more complex when the axial dispersion phenomena are coupled with external film diffusion resistance and intraparticle diffusion resistance; the analytical solutions are sometimes obtainable, but they are frequently expressed in terms of slowly convergent series, or contain higher transcendental functions that have to be evaluated numerically via proper subroutines. In this case, it will take a long time to calculate the breakthrough curves; also, making a program to obtain numerical values is not easy, so it is desirable to have a method that is easy to program and also allows rapid computation of breakthrough curves for typical models of fixed-bed adsorbers.

Generally, two methods can be used to simplify the mathematical model for fixed-bed adsorbers. One is to use the parabolic concentration profile assumption in the adsorbent (Liaw et al., 1979; Rice, 1982; Cen and Yang, 1986); the other is to simulate the impulse response, and by means of the convolution theorem to get the solution for a step response, that is, the breakthrough curve (Wiedemann et al., 1978; Razavi et al., 1978; Linek and Dudukovic, 1982; Wang and Lin, 1986).

For impulse-response experiments, moment analysis is often used for parameter estimation (Schneider and Smith, 1968; Suzuki and Smith, 1971), since the first few moments of the impulse response usually contain all the parameters of the system. Therefore, a solution that utilizes moments for predicting breakthrough curves is of particular interest. Such an approach was first suggested by Wiedemann et al. (1978) and Razavi et al. (1978) at almost the same time. Linek and Dudukovic (1982) also obtained an approximation in terms of a Laguerre polynomial series expansion of the impulse response. Recently, Wang and Lin (1986) used a quasi-lognormal probability density function to simulate the impulse response, and tested their solutions with the exact solutions given in the literature. This method is a simple and handy one, but it is not well known, since the original paper appeared in Chinese.

Correspondence concerning this article should be addressed to G. H. Xiu.

Many theoretical and experimental investigations have been reported in the literature for spherical adsorbents. Although a certain amount of information has appeared on experimental breakthrough curves for fixed-bed adsorbers packed with activated-carbon fiber (for activated-carbon fiber, the L/D ratio is large; it can be assumed to be cylinders of infinite length) (Yang et al., 1993), the theoretical research on breakthrough curves has received comparatively less attention (Xiu, 1996).

The objective of this work is to introduce the quasi-lognormal distribution (Q-LND) approximation, first suggested by Wang and Lin (1986), which takes into account axial dispersion, external film diffusion resistance, and intraparticle diffusion resistance to predict the breakthrough curves for three different geometries: a slab, a cylinder, and a sphere, and to compare the solution with the exact solution and the parabolic-profile approximation in accuracy and computation time; further, to point out the validity and limitation of the Q-LND approximation.

Another objective of this work is to study the effect of particle geometries on the breakthrough curves, to explore the conditions where one should consider this effect on breakthrough curves.

Theoretical Studies

Here we consider an isothermal adsorption column packed with porous particles. At time zero, a step change in the concentration of an adsorbate was introduced to a flowing stream. The adsorption column was subjected to axial dispersion, external film diffusion resistance, and intraparticle diffusion resistance. The following assumptions are presumed in the analysis:

1. The temperature is essentially constant throughout the column;
2. Fick's Law of Diffusion governs axial dispersion in the bulk fluid phase within the column;
3. The adsorption isotherm is linear;
4. Fick's Law of Diffusion governs transport within the adsorbent particles;
5. The axial fluid velocity in the column is constant.

The first condition is satisfied in liquid-adsorption systems in which the heat of adsorption is small compared to the heat capacity of the solvent. It is approximated in a gas-adsorption system only when the feed gas is highly diluted in the adsorbate (Liaw et al., 1979). The last condition is justified provided the concentration of the adsorbable species is sufficiently small, that is, for a trace component in an inert carrier (Ruthven, 1984).

Based on the preceding assumptions, the fixed-bed adsorber can be described by the following set of equations:

$$D_L\frac{\partial^2 C}{\partial Z^2}-u\frac{\partial C}{\partial Z}-\frac{\partial C}{\partial t}-\frac{1-\alpha}{\alpha}\rho_p\frac{\partial \bar{q}}{\partial t}=0 \tag{1}$$

$$\frac{\partial q}{\partial t}=D_s\left(\frac{\partial^2 q}{\partial r^2}+\frac{p}{r}\frac{\partial q}{\partial r}\right). \tag{2}$$

The initial and boundary conditions are

$$C(0,t)=C_0 \tag{3}$$

$$C(\infty,t)=0 \tag{4}$$

$$C(Z,0)=0 \tag{5}$$

$$\left(\frac{\partial q}{\partial r}\right)_{r=0}=0 \tag{6}$$

$$q(r,Z,0)=0 \tag{7}$$

$$\rho_p\frac{\partial \bar{q}}{\partial t}=\frac{p+1}{R}k_f\left(C-\frac{q_s}{K}\right), \tag{8}$$

where

$$q_s(Z,t)=q(R,Z,t) \tag{9}$$

$$\bar{q}=\frac{p+1}{R^{p+1}}\int_0^R q(r,Z,t)r^p\,dr \tag{10}$$

in which p is the shape factor of the adsorbent particle, $p=2$ for sphere, $p=1$ for cylinder, and $p=0$ for slab.

The following dimensionless quantities are introduced:

$x=q/KC_0,\ y=C/C_0$	dimensionless concentrations
$\zeta=Z/L$	dimensionless axial distance
$\xi=r/R$	dimensionless radial distance
$\theta=LD_s/uR^2$	bed-length parameter
$\delta=K\rho_p/m$	distribution ratio
$Pe=uL/D_L$	Peclet number based on adsorber length
$Bi=k_fR/K\rho_pD_s$	modified Biot number
$\tau=tD_s/R^2$	dimensionless contact time.

Written in dimensionless form, Eqs. 1–10 become:

$$\frac{1}{Pe}\frac{\partial^2 y}{\partial \zeta^2}-\frac{\partial y}{\partial \zeta}-\theta\frac{\partial y}{\partial \tau}-\theta\delta\frac{\partial \bar{x}}{\partial \tau}=0 \tag{11}$$

$$\frac{\partial x}{\partial \tau}=\frac{\partial^2 x}{\partial \xi^2}+\frac{p}{\xi}\frac{\partial x}{\partial \xi} \tag{12}$$

$$y(0,\tau)=1 \tag{13}$$

$$y(\infty,\tau)=0 \tag{14}$$

$$y(\zeta,0)=0 \tag{15}$$

$$\left(\frac{\partial x}{\partial \xi}\right)_{\xi=0}=0 \tag{16}$$

$$x(\xi,\zeta,0)=0 \tag{17}$$

$$\frac{\partial \bar{x}}{\partial \tau}=(1+p)Bi(y-x_s) \tag{18}$$

$$x_s(\zeta,\tau)=x(1,\zeta,\tau) \tag{19}$$

$$\bar{x}=(1+p)\int_0^1 x(\xi,\zeta,\tau)\xi^p\,d\xi. \tag{20}$$

By solving Eq. 12 for the special case that $x_s=1$, denoted by $U(\xi,\tau)$, and applying Duhamel's theorem to the solution, the

Table 1. Expressions of $f(\xi, \lambda_n)$ and λ_n in Eq. 22

p	$f(\xi, \lambda_n)$	$\lambda_n\ (n=1, 2, 3, \ldots)$
2	$(-1)^{n+1}\sin(\sqrt{\lambda_n}\,\xi)/\xi$	$n^2\pi^2$
1	$J_0(\sqrt{\lambda_n}\,\xi)/J_1(\sqrt{\lambda_n})$	λ_n given by $J_0(\sqrt{\lambda_n})=0$*
0	$(-1)^{n+1}\cos(\sqrt{\lambda_n}\,\xi)$	$[(2n-1)/2]^2\pi^2$

*J_0 is the Bessel function of order zero. The first eight roots of $J_0(\sqrt{\lambda_n})=0$ are $\sqrt{\lambda}=2.4048, 5.5201, 8.6537, 11.7915, 14.9309, 18.0711, 21.2116, 24.3525$ (Olver, 1970). It should be noted that at large values of n the difference $\sqrt{\lambda_{n-1}}-\sqrt{\lambda_n}$ is close to π.

expression for $x(\xi,\zeta,\tau)$ is then given in terms of the surface concentration $x_s(\zeta,\tau)$:

$$x(\xi,\zeta,\tau)=\int_0^{\tau} x_s(\zeta,\lambda)\frac{\partial}{\partial\tau}U(\xi,\tau-\lambda)\,d\lambda, \qquad (21)$$

where

$$U(\xi,\tau)=1-2\sum_{n=1}^{\infty}\frac{f(\xi,\lambda_n)}{\sqrt{\lambda_n}}\exp(-\lambda_n\tau). \qquad (22)$$

The $f(\xi,\lambda_n)$ and λ_n for $p=0$ and 1 are derived in the present work and are summarized in Table 1 along with the results for $p=2$ (Rosen, 1952). Following Rosen (1952) and Rasmuson and Neretnieks (1980), the time-domain solution of y is

$$y=\frac{1}{2}+\frac{1}{\pi}\int_0^{\infty}\exp\left(\frac{Pe}{2}\zeta-\zeta\sqrt{\frac{\sqrt{a^2+b^2}+a}{2}}\right)\times\sin\left(\beta\tau-\zeta\sqrt{\frac{\sqrt{a^2+b^2}-a}{2}}\right)\frac{d\beta}{\beta}, \qquad (23)$$

where

$$a=\frac{1}{4}Pe^2+\theta\delta Pe(1+p)H_1 \qquad (24)$$

$$b=\theta Pe[\beta+\delta(1+p)H_2] \qquad (25)$$

$$H_1=\frac{Bi^2H_{D1}+Bi(H_{D1}^2+H_{D2}^2)}{(Bi+H_{D1})^2+H_{D2}^2} \qquad (26)$$

$$H_2=\frac{Bi^2H_{D2}}{(Bi+H_{D1})^2+H_{D2}^2} \qquad (27)$$

$$H_{D1}=2\sum_{n=1}^{\infty}\frac{\beta^2}{\beta^2+\lambda_n^2} \qquad (28)$$

$$H_{D2}=2\sum_{n=1}^{\infty}\frac{\lambda_n\beta}{\beta^2+\lambda_n^2}. \qquad (29)$$

For $\beta \ll \lambda_1$, Eqs. 28 and 29 can be simplified as

$$H_{D1}=\frac{\beta^2}{(1+p)^2(3+p)} \qquad (\beta\ll\lambda_1;\ p=0,1,2) \qquad (30)$$

$$H_{D2}=\frac{\beta}{1+p} \qquad (\beta\ll\lambda_1;\ p=0,1,2). \qquad (31)$$

Further, for $p=0$ and 2, the trigonometric expressions of Eqs. 28 and 29 can be obtained. For $p=2$, see the work of Rosen (1952). The results for $p=0$ are given as follows:

$$H_{D1}=\lambda\left(\frac{\sinh 2\lambda-\sin 2\lambda}{\cosh 2\lambda+\cos 2\lambda}\right) \qquad (p=0) \qquad (32)$$

$$H_{D2}=\lambda\left(\frac{\sinh 2\lambda+\sin 2\lambda}{\cosh 2\lambda+\cos 2\lambda}\right) \qquad (p=0), \qquad (33)$$

in which $\lambda=\sqrt{\beta/2}$.

For high values of Pe ($D_L\to 0$), we can disregard all terms of order $1/Pe$, and Eq. 23 becomes

$$y=\frac{1}{2}+\frac{1}{\pi}\int_0^{\infty}\exp[-\delta\theta(1+p)H_1\zeta]\times\sin\{\beta\tau-\zeta\theta[\beta+\delta(1+p)H_2]\}\frac{d\beta}{\beta}. \qquad (34)$$

The model, together with its general solution (Eqs. 1–34), follows the approach of Rasmuson and Neretnieks (1980) with two important improvements. First, the model is put into dimensionless form, which makes the model more general. Second, the model is generalized for the three particle shapes for which analytical solutions are derived—slab, cylinder, and sphere. Previous studies are limited only to the sphere adsorbents.

Parabolic-profile approximation

In order to reduce the complexity of the exact solution, parabolic concentration profiles in the adsorbent have been assumed in some previous studies of breakthrough curves (Liaw et al., 1979; Rice, 1982; Cen and Yang, 1986). (These studies also assumed no axial dispersion, so their solutions are not relevant to the present work.) In the present work, we use the following parabolic-profile assumption for any cases of Pe:

$$x(\xi,\zeta,\tau)=a_0(\zeta,\tau)+a_2(\zeta,\tau)\xi^2. \qquad (35)$$

Applying the boundary conditions, along with the definition of volume-averaged x, $\bar{x}$, we obtain

$$\frac{\partial x}{\partial\xi}=\frac{1}{H_{D3}}(y-\bar{x}) \qquad \text{at } \xi=1, \qquad (36)$$

where

$$H_{D3}=\frac{1}{Bi}+\frac{1}{3+p}. \qquad (37)$$

When the governing diffusion equation (Eq. 12) is volume-averaged, we have

$$\frac{\partial \bar{x}}{\partial \tau} = (1+p)\frac{\partial x}{\partial \xi} \qquad \text{at } \xi = 1. \tag{38}$$

The time-domain solution for the parabolic-profile assumption is the same as Eqs. 23–25, in which

$$H_1 = \frac{\beta^2 H_{D3}}{(1+p)^2 + \beta^2 H_{D3}^2} \tag{39}$$

$$H_2 = \frac{(1+p)\beta}{(1+p)^2 + \beta^2 H_{D3}^2}. \tag{40}$$

When the contribution of axial dispersion is negligible, that is, $Pe \to \infty$, the parabolic profile approximation can be expressed as (Rice, 1980)

$$y = 1 - \int_0^{\eta} \exp(-\nu - \beta) I_0\left(\sqrt{4\nu\beta}\right) d\beta, \tag{41}$$

where

$$\eta = (1+p)\delta\zeta\theta/H_{D3}, \tag{42}$$

$$\nu = (1+p)(\tau - \zeta\theta)/H_{D3}, \tag{43}$$

and I_0 is the modified Bessel function of order zero.

Quasi-lognormal distribution approximation

Wiedemann et al. (1978), Razavi et al. (1978), and Linek and Dudukovic (1982) approximated the breakthrough curves for fixed-bed adsorbers using the moments of the impulse response in terms of an orthogonal polynomial series expansion. Wang and Lin (1986) assumed that the quasi-lognormal (Q-LND) probability density function, $y_\delta(\tau)$, can be used to represent the impulse response of the system, where $y_\delta(\tau)$ is the product of the lognormal probability density function and the zeroth moment of the impulse response of the system, μ_0, that is,

$$y_\delta(\tau) = \frac{\mu_0}{\sqrt{2\pi}\sigma\tau} \exp\left[-\frac{(\ln\tau - \mu)^2}{2\sigma^2}\right]. \tag{44}$$

The first absolute moment, m_1, and the second central moment, m'_2 of Eq. 44 in the τ-domain are given as follows:

$$m_1 = \exp\left(\mu + \frac{\sigma^2}{2}\right) \tag{45}$$

$$m'_2 = \exp(2\mu + \sigma^2)[\exp(\sigma^2) - 1]. \tag{46}$$

For our system, the fundamental dimensionless equations employed for impulse input are essentially the same as Eqs. 11–20 if Eq. 13 is replaced by

$$y(0,0) = 1. \tag{47}$$

According to the work of Suzuki and Smith (1971), the expressions of μ_0, the first absolute moment, μ_1, and the second central moment, μ'_2, for the impulse-input system can be obtained as

$$\mu_0 = 1 \tag{48}$$

$$\mu_1 = \zeta\theta(1+\delta) \tag{49}$$

$$\mu'_2 = \zeta\theta\left[\frac{2}{1+p}\delta H_{D3} + \frac{2\theta}{Pe}(1+\delta)^2\right]. \tag{50}$$

If $y_\delta(\tau)$ represents the impulse response of the system, m_1 and m'_2 of Eq. 44 should be equal to the first absolute moment, μ_1, and the second central moment, μ'_2, respectively. Then the following expressions of μ and σ in terms of μ_1 and μ'_2 can be obtained from Eqs. 45 and 46:

$$\mu = \ln\mu_1 - \frac{1}{2}\ln\left(1 + \frac{\mu'_2}{\mu_1^2}\right) \tag{51}$$

$$\sigma = \left[\ln\left(1 + \frac{\mu'_2}{\mu_1^2}\right)\right]^{1/2}. \tag{52}$$

The approximation to a step response, that is, the breakthrough curve, $y(\tau)$, is obtained by using the convolution integral of the impulse response, $y_\delta(\tau)$, or

$$y(\tau) = \int_0^{\tau} y_\delta(\beta)\, d\beta. \tag{53}$$

By combining Eq. 53 with Eq. 44, the analytical expression of the Q-LND approximation, in which only three moments of the impulse response appear, can be obtained as follows:

$$y(\tau) = \mu_0 \int_{-\infty}^{(\ln\tau - \mu)/\sigma} \frac{1}{\sqrt{2\pi}} \exp\left(-\frac{\beta^2}{2}\right) d\beta. \tag{54}$$

Results and Discussion

The Q-LND approximation, Eq. 54 together with Eqs. 48–52, will be compared with the exact solution, Eqs. 23–29, and the parabolic-profile approximation, Eqs. 23–25 together with Eqs. 37, 39, and 40, under the condition of $\zeta = 1$, $\delta = K\rho_p/m = 5\times10^3$. The effects of parameters Bi, Pe, θ, and the shape factor p on the breakthrough curves will be discussed.

$\zeta = 1$ is the point at which the breakthrough curve is measured, that is, the outlet of the column. The packed-bed porosity α is known to be in the range 0.35–0.45 (Drew et al., 1950) for spherical particles and in the range of 0.7–0.9 for long, cylindrical particles, such as activated-carbon fiber. Realistic values of K cover an extremely wide range. Therefore, using 5×10^3 for $\delta = K\rho_p/m$ in the test calculations is reasonable.

Figures 1–4 show the effects of Bi and the shape factor p on $y-\tau$ curves calculated from the Q-LND approximation (Q-LND; dotted-broken line), the exact solution (EXACT; solid line), and the parabolic profile approximation (PARABOLIC; broken line), respectively, at $Pe = 10^2$ for three values of θ.

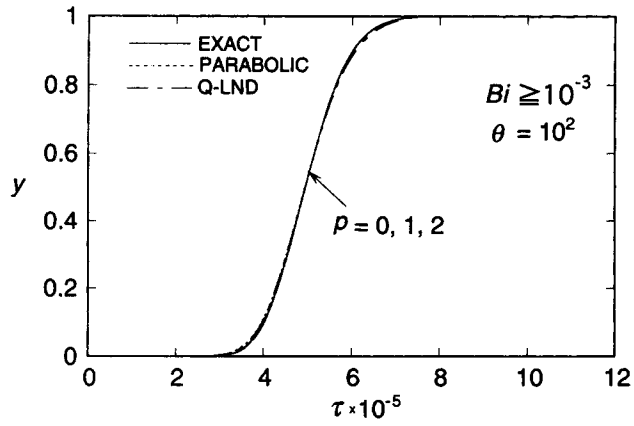

Figure 1. Effects of Bi ($Bi \geq 10^{-3}$) and p ($p = 0$, 1, and 2) on y-τ curves at $Pe = 10^2$ for $\theta = 10^2$.

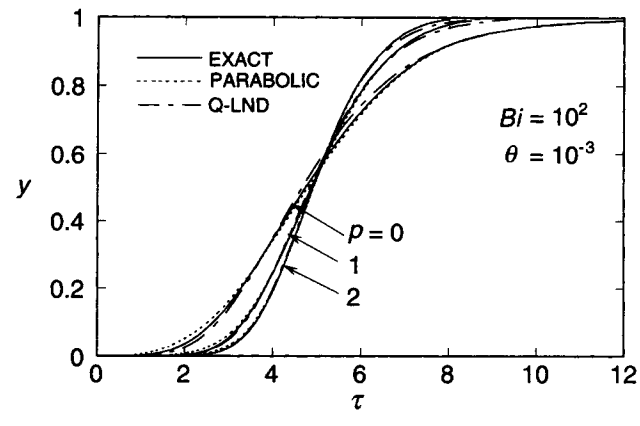

Figure 3. Effects of Bi ($Bi = 10^2$) and p ($p = 0$, 1, and 2) on y-τ curves at $Pe = 10^2$ for $\theta = 10^{-3}$.

The parameter Bi stands for the ratio of the internal resistance to the external resistance for mass transfer, and the parameter θ is the ratio of the residence time of fluid in the adsorber to the diffusion time of adsorbate into the adsorbent. Figures 1 and 2 show $y - \tau$ curves for long columns, $\theta = 10^2$ and $\theta = 1$, respectively. In the two figures, the EXACT curves for different p nearly coincide with each other when Bi is larger than a certain small number, 10^{-3} in the case of Figure 1 and 10^{-1} in the case of Figure 2. The PARABOLIC and the Q-LND curves are very close to the EXACT curves, which indicates that the parabolic-profile approximation and the Q-LND approximation are satisfactory for representing the exact solution of the breakthrough curve for long columns.

In the case of a short column ($\theta = 10^{-3}$, as shown in Figures 3 and 4), the EXACT lines differ with different values of p in the two cases of different Bi, that is, $Bi = 10^2$ (Figure 3) and $Bi = 0.5$ (Figure 4). When $Bi = 10^2$ (where the internal mass transfer is a significant resistance), the Q-LND lines are close to the corresponding EXACT lines as well as the PARABOLIC lines. On the other hand, when Bi is small as 0.5 (Figure 4), all the Q-LND lines differ significantly from the EXACT lines, though the PARABOLIC lines are close to the EXACT lines. Therefore, the Q-LND approximation is not acceptable in the case where both θ and Bi are small. Later, we give an empirical criterion for the applicability of the Q-LND approximation.

It is noted here that for a short column, especially in Figure 3, the breakpoint for the curve of $p = 2$ comes later than those for the other two curves. The outer surface per unit volume of adsorbent becomes larger in the order of $p = 0$, 1, and 2. Therefore, increasing the outer surface is of advantage for retarding the breakpoint of the breakthrough curve for a short column.

Figures 5 and 6 show the effect of Pe on the breakthrough curves for long and short columns. In the case that $\theta = 1$ (Figure 5), the EXACT curves differ for different p when Pe is as large as 10^3. On the other hand, when Pe is as small as 2, that is, the backmixing of the fluid is significant, the EXACT, the PARABOLIC, and the Q-LND lines differ slightly for three values of p. In this case, the breakpoint occurs quickly, but the Q-LND approximation is acceptable, though the agreement is not as good as in the case where $Pe = 10^3$.

For a short column ($\theta = 10^{-3}$) with $Bi = 10^2$, as shown in Figure 6, the influence of Pe on the breakthrough curves is almost the same as in Figure 5; that is, when Pe is large, the shape factor p affects the shape of the $y - \tau$ curves, though not when Pe is as small as 1. In the latter case, the Q-LND approximation is also acceptable for representing the breakthrough curve, though it is not satisfactory.

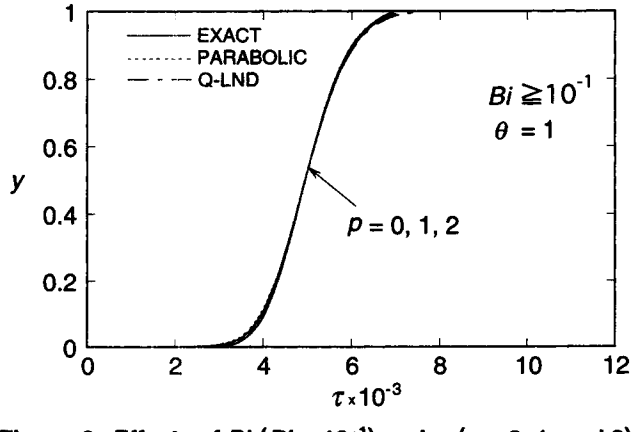

Figure 2. Effects of Bi ($Bi \geq 10^{-1}$) and p ($p = 0$, 1, and 2) on y-τ curves at $Pe = 10^2$ for $\theta = 1$.

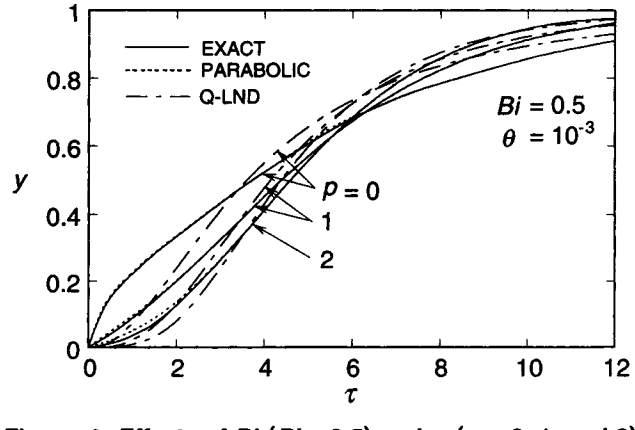

Figure 4. Effects of Bi ($Bi = 0.5$) and p ($p = 0$, 1, and 2) on $y - \tau$ curves at $Pe = 10^2$ for $\theta = 10^{-3}$.

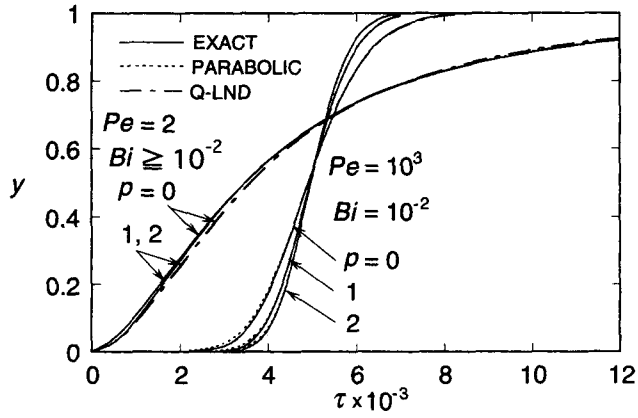

Figure 5. Effects of *Pe* (*Pe* = 2 and 10^3) and *p* (*p* = 0, 1, and 2) on *y*-τ curves at *Bi* $\geq 10^{-2}$ for $\theta = 1$.

We have shown typical cases where (1) the shape factor p does or does not have an influence, and (2) the Q-LND approximation is acceptable or not acceptable. Let us discuss the criteria for the two cases by using the expressions obtained in the Q-LND approximation.

According to Eq. 54, the breakthrough curves are determined by the two dimensionless parameters, μ_1 and μ_2'/μ_1^2. The expression of μ_2'/μ_1^2, in terms of parameters Bi, θ, δ, p, and Pe, can be obtained from Eqs. 49 and 50 as

$$\frac{\mu_2'}{\mu_1^2} = \left(\frac{\mu_2'}{\mu_1^2}\right)_{\rm I} + \left(\frac{\mu_2'}{\mu_1^2}\right)_{\rm II}, \tag{55}$$

where

$$\left(\frac{\mu_2'}{\mu_1^2}\right)_{\rm I} = \frac{2H_{D3}}{\theta(1+\delta)(1+p)} \tag{56}$$

$$\left(\frac{\mu_2'}{\mu_1^2}\right)_{\rm II} = \frac{2}{Pe}, \tag{57}$$

in which we presumed that $\zeta = 1$ and $\delta \gg 1$.

The second term contains only Pe while the combined particle mass-transfer coefficient H_{D3}, shape factor p, and $\theta(1+\delta)$ are involved in the first term. The two expressions of

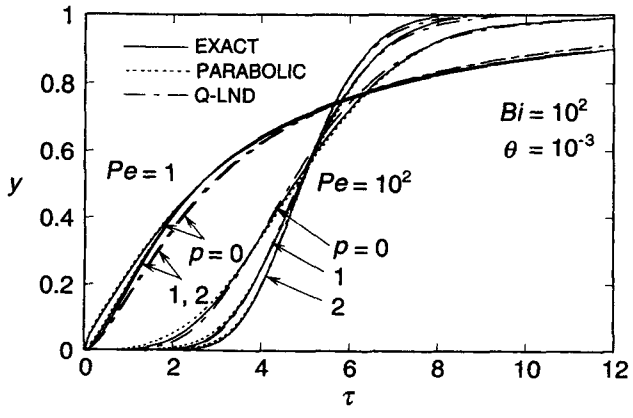

Figure 6. Effects of *Pe* (*Pe* = 1 and 10^2) and *p* (*p* = 0, 1, and 2) on *y*-τ curves at *Bi* = 10^2 for $\theta = 10^{-3}$.

Table 2. Contributions of $(\mu_2'/\mu_1^2)_{\rm I}$ and $(\mu_2'/\mu_1^2)_{\rm II}$ on μ_2'/μ_1^2 for $p = 2$

Figure	*Pe*	θ	*Bi*	$(\mu_2'/\mu_1^2)_{\rm I}$	$(\mu_2'/\mu_1^2)_{\rm II}$	μ_1
1	10^2	10^2	10^{-3}	1.3×10^{-3}	2×10^{-2}	5×10^5
2	10^2	1	10^{-1}	1.3×10^{-3}	2×10^{-2}	5×10^3
3	10^2	10^{-3}	10^2	2.8×10^{-2}	2×10^{-2}	5
4	10^2	10^{-3}	0.5	0.293	2×10^{-2}	5
5	10^3	1	10^{-2}	1.3×10^{-2}	2×10^{-3}	5×10^3
	2	1	10^{-2}	1.3×10^{-2}	1	5×10^3
6	10^2	10^{-3}	10^2	2.8×10^{-2}	2×10^{-2}	5
	1	10^{-3}	10^2	2.8×10^{-2}	2	5

$(\mu_2'/\mu_1^2)_{\rm I}$ are obtained for the extreme value of Bi as follows: (1) when $Bi \ll 3+p$, then $H_{D3} \approx 1/Bi$; therefore,

$$\left(\frac{\mu_2'}{\mu_1^2}\right)_{\rm I} = \frac{2}{Bi\,\theta(1+\delta)(1+p)}; \tag{58}$$

(2) when $Bi \gg 3+p$, then $H_{D3} \approx 1/(3+p)$, which results in

$$\left(\frac{\mu_2'}{\mu_1^2}\right)_{\rm I} = \frac{2}{\theta(1+\delta)(1+p)(3+p)}. \tag{59}$$

Case 1 (i.e., $Bi \ll 3+p$) occurs only for strong adsorption (Do and Rice, 1990), since a typical value of Bi is greater than 1.

Table 2 provides a summary of dimensionless parameters $(\mu_2'/\mu_1^2)_{\rm I}$, $(\mu_2'/\mu_1^2)_{\rm II}$, and μ_1 together with Bi, θ, and Pe corresponding to Figures 1–6 only in the case where $p = 2$.

When the term $(\mu_2'/\mu_1^2)_{\rm II}$ is larger than the first, where the column is long or Pe is extraordinarily small, the shape factor p does not influence the breakthrough curves as shown in Figures 1, 2, 5 ($Pe = 2$) and 6 ($Pe = 1$). On the other hand, when the term $(\mu_2'/\mu_1^2)_{\rm I}$ is larger than the second, the shape factor p must be taken into consideration in representing the breakthrough curves, as shown in Figures 3, 4, 5 ($Pe = 10^3$) and 6 ($Pe = 10^2$). Therefore, the effect of the shape factor p on the breakthrough curves should be taken into account when

$$(\mu_2'/\mu_1^2)_{\rm I} > (\mu_2'/\mu_1^2)_{\rm II}. \tag{60}$$

As for the criterion of the applicability of the Q-LND approximation, we have found an inequality:

$$(\mu_2'/\mu_1^2)_{\rm I} < 0.1 \tag{61}$$

by comparing the breakthrough curves calculated from the exact solution and the Q-LND approximation.

It is interesting to note that the Q-LND approximation can represent the breakthrough curve fairly well when $(\mu_2'/\mu_1^2)_{\rm II}$ is large (Pe is small), if the inequality (61) is satisfied, as shown in Figures 5 ($Pe = 2$) and 6 ($Pe = 1$). However, if the inequality (61) is not satisfied, as in the case of Figure 4, the Q-LND approximation fails to represent the breakthrough curve, even though the second term $(\mu_2'/\mu_1^2)_{\rm II}$ is small.

The calculation speed of the Q-LND approximation is more than two orders of magnitude faster than the parabolic profile approximation, and the latter is almost the same order of magnitude as that of the exact solution, as shown in Table 3.

Table 3. Computation Time Required: Q-LND Approximation, Parabolic Profile Approximation, and Exact Solution for $\delta = 5 \times 10^3$

Parameter Values		p	Computation Time Required in Compag 5133 (10 points) Q-LND s	Exact s	Parabolic s
$Bi = 10$		0	0.03*	32	17
$Pe = 10^2$	Figure 2	1	0.03	64	17
$\theta = 1$		2	0.03	32	17
$Bi = 10^2$		0	0.03	47	16
$Pe = 10^2$	Figure 3	1	0.03	380	16
$\theta = 10^{-3}$		2	0.03	47	16
$Bi = 10$		0	0.03	39	21
$Pe = 2$	Figure 5	1	0.03	74	21
$\theta = 1$		2	0.03	39	21

*For Q-LND approximation, the display of results is the time-controlling step: the time of 10-point calculation is only 280 μs.

The reason is that the Q-LND approximation is easy to calculate with a polynomial approximation (Zelen and Severo, 1970). For the parabolic-profile approximation and the exact solution, Eq. 23 is a slowly converging oscillating integral involving the product of an exponentially decaying function and a periodic sine function. The integration should be performed over each half-period of the sine wave (Rasmuson, 1985). Therefore, we need experience and skill to obtain the correct numerical values of both the exact solution and the parabolic approximation. The Q-LND approximation seems best suited for this point of numerical calculation.

Conclusions

Based on the work of Wang and Lin (1986), the quasi-lognormal distribution (Q-LND) approximation was derived for fixed-bed adsorbers by taking into account axial dispersion, external film diffusion resistance, and intraparticle diffusion resistance for slab, cylindrical and spherical absorbent-particle geometries. The exact solution and the parabolic-profile approximation were also obtained for different particle geometries.

The results show that the Q-LND approximation is a simple and acceptable solution. It predicts breakthrough curves with an accuracy comparable to the parabolic-profile approximation over a wide range of parameters. Compared with the latter, it only takes less than one hundredth computation time and does not have a convergence problem in numerical calculations. A criterion for the applicability of the Q-LND approximation has been suggested.

The effect of the particle geometries on the breakthrough curves is discussed. A criterion is also provided for the Q-LND approximation to explore the conditions where one should consider this effect on breakthrough curves.

Notation

C = concentration in fluid, kg/m^3
C_0 = inlet concentration in fluid, kg/m^3
D_L = longitudinal dispersion coefficient, m^2/s
D_s = diffusivity in solid phase, m^2/s
k_f = fluid-to-particle mass-transfer coefficient, m/s
K = adsorption equilibrium constant, m^3/kg
L = length of column, m
$m = \alpha/(1-\alpha)$
q = internal concentration in particles, kg/kg
$\bar{q}$ = volume-averaged internal concentration in particle, kg/kg
r = radial distance from center of particle, m
R = characteristic particle dimension: half-thickness ($p = 0$); radius ($p = 1$ or 2), m
t = time, s
u = average velocity in the interparticle space in the column, m/s
$\bar{x}$ = dimensionless volume-averaged internal concentration in particle = $(\bar{q}/KC_0)$
Z = axial distance from column entrance, m
β = integration parameter
μ = parameter, defined in Eq. 44
ρ_p = density of porous particle, kg/m^3
σ = parameter, defined in Eq. 44

Literature Cited

Cen, P. L., and R. T. Yang, "Analytic Solution for Adsorber Breakthrough Curves with Bidisperse Sorbents (Zeolites)," *AIChE J.*, **32**, 1635 (1986).

Do, D. D., and R. G. Rice, "Applicablity of the External-Diffusion Model in Adsorption Studies," *Chem. Eng. Sci.*, **45**, 1419 (1990).

Drew, T. B., H. H. Dunkle, and R. P. Generaux, "Flow of Fluids," *Chemical Engineers' Handbook*, 3rd ed., J. H. Perry, ed., McGraw-Hill, New York, p. 394 (1950).

Liaw, C. H., J. S. P. Wang, R. A. Greenkorn, and K. C. Chao, "Kinetics of Fixed-Bed Adsorption: A New Solution," *AIChE J.*, **25**, 376 (1979).

Linek, F., and M. P. Dudukovic, "Representation of Breakthrough Curves for Fixed-Bed Adsorbers and Reactors Using Moments of the Impulse Response," *Chem. Eng. J.*, **23**, 31 (1982).

Masamune, S., and J. M. Smith, "Adsorption Rate Studies—Interaction of Diffusion and Surface Processes," *AIChE J.*, **11**, 34 (1965).

Olver, F. W. J., "Bessel Functions of Integer Order," *Handbook of Mathematical Functions*, M. Abramowitz and I. A. Stegun, eds., Dover, New York, p. 409 (1970).

Rasmuson, A., "Exact Solution of a Model for Diffusion in Particles and Longitudinal Dispersion in Packed Beds: Numerical Evaluation," *AIChE J.*, **31**, 518 (1985).

Rasmuson, A., and I. Neretnieks, "Exact Solution of a Model for Diffusion in Particles and Longitudinal Dispersion in Packed Beds," *AIChE J.*, **26**, 686 (1980).

Razavi, M. S., B. J. McCoy, and R. G. Carbonell, "Moment Theory of Breakthrough Curves for Fixed-Bed Adsorbers and Reactors," *Chem. Eng. J.*, **16**, 211 (1978).

Rice, R. G., Letter to the Editors, *AIChE J.*, **26**, 334 (1980).

Rice, R. G., "Approximate Solution for Batch, Packed Tube and Radial Flow Adsorption—Comparison with Experiment," *Chem. Eng. Sci.*, **37**, 83 (1982).

Rosen, J. B., "Kinetics of a Fixed Bed System for Solid Diffusion into Spherical Particles," *J. Chem. Phys.*, **20**, 387 (1952).

Ruthven, D. M., *Principles of Adsorption & Adsorption Processes*, Wiley, New York, p. 231 (1984).

Schneider, P., and J. M. Smith, "Adsorption Rate Constants from Chromatography," *AIChE J.*, **14**, 762 (1968).

Suzuki, M., and J. M. Smith, "Kinetic Studies by Chromatography," *Chem. Eng. Sci.*, **26**, 221 (1971).

Wang, C. T., and C. Lin, "Prediction of Breakthrough Curves for Fixed Beds," *Hua Gong Xue Bao (China)*, **37**, 183 (1986).

Wiedemann, K., A. Roethe, K. H. Radeke, and D. Gelbin, "The Modeling of Adsorption-Desorption Breakthrough Curves Using Statistical Moments," *Chem. Eng. J.*, **16**, 19 (1978).

Xiu, G. H., "Modeling Breakthrough Curves in a Fixed-Bed of Activated Carbon Fiber—Exact Solution and Parabolic Approximation," *Chem. Eng. Sci.*, **51**, 4039 (1996).

Yang, O. B., J. C. Kim, J. S. Lee, and Y. J. Kim, "Use of Activated Carbon Fiber for Direct Removal of Iodine from Acetic Acid Solution," *Ind. Eng. Chem. Res.*, **32**, 1692 (1993).

Zelen, M., and N. C. Severo, "Probability Functions," *Handbook of Mathematical Functions*, M. Abramowitz and I. A. Stegun, eds., Dover, New York, p. 932 (1970).

Manuscript received July 1, 1996, and revision received Oct. 15, 1996.